Application of High Precision Two-Way S-band Ranging to the Navigation of the Galileo Earth Encounters

Vincent M. Pollmeier[1], Pieter H. Kallemeyn[1], and Sam W. Thurman[2]

The application of high-accuracy S/S-band (2.1 GHz uplink/ 2.3 GHz downlink) ranging to orbit determination with relatively short data arcs is investigated for the approach phase of each of the Galileo spacecraft's two Earth encounters (8 December 1990 and 8 December 1992). Analysis of S-band ranging data from Galileo indicated that under favorable signal levels meter level precision was attainable. It is shown that ranging data of sufficient accuracy, when acquired from multiple stations, can sense the geocentric angular position of a distant spacecraft, Explicit modeling of ranging bias parameters for each station pass is used to largely remove systematic ground system calibration errors and transmission media effects from the Galileo range measurements, which would otherwise corrupt the angle finding capabilities of the data. The accuracy achieved using the precision range filtering strategy proved markedly better when compared to post-flyby reconstructions than did solutions utilizing a traditional Doppler/range filter strategy. In addition, the navigation accuracy achieved with precision ranging was comparable to that obtained using delta-Differenced One-Way Range (ΔDOR), an interferometric measurement of spacecraft angular position relative to a natural radio source, which was also used operationally.

INTRODUCTION

The approach phases leading up to the Galileo spacecraft's two Earth encounters (designated E1 and E2) provided invaluable opportunities to test the viability of high-precision two-way ranging as an operational radiometric data type. Ranging data from NASA's Deep Space Network (DSN) has been accurate to better than 15 m for more than two decades under favorable radio link conditions. Such data have typically been utilized at assumed data accuracies of 100 - 10000 m, due to the effects of ranging system calibration errors and inadequately modeled spacecraft nongravitational accelerations[3]. Improvements in the accuracy and stability of timing systems, ranging system calibration techniques, and transmission media calibrations, when utilized with more sophisticated orbit determination software, now make it possible to reconsider the use of precision range for interplanetary spacecraft. Other recent experimental attempts to utilize high precision range with the Ulysses spacecraft [1] have met with success. Presented here are the results of an application of the same filter strategy to the navigation of both of the Galileo Earth encounters. In many ways the Galileo encounters are an ideal test of this strategy. Due to the relatively small Earth-spacecraft range, the radio link performance is

[1] Member Technical Staff, Navigation Systems Section, Jet Propulsion laboratory, California Institute of Technology, 4800 Oak Grove Drive, Pasadena, CA 91109; Member AAS

[2] Technical Manager, Navigation Systems Section, Jet Propulsion Laboratory; Member AAS

[3] Data weights quoted here are one-way equivalent data weights. The actual precision of the two way observable is roughly twice the quoted data weight.

good and extremely accurate post-flyby knowledge is available to allow for validation of the results.

The analysis considers the approach navigation prior' 10 the final maneuver' for each of the Galileo spacecraft's two Earth encounters. The Galileo spacecraft was launched from the space shuttle on 18 October 1989. lacking the launch energy for a direct Jupiter trajectory, the spacecraft was targeted for a Venus flyby, which redirected the spacecraft for an Earth flyby on 8 December 1990. This flyby put the spacecraft on a two year elliptical orbit, out through the asteroid belt anti back past the Earth on 8 December 1992. This final gravity assist placed the spacecraft on a trajectory to Jupiter, with a planned arrival date of 7 December 199S. Due to Earth navigation constraints, at no time during the approach to either Earth encounter could the probability of the spacecraft impacting the Earth exceed 1 x 1()-6. For this reason, a series of deterministic targeting maneuvers were performed during the Earth approach phase. The final targeting maneuvers were performed at ii-60 days and E-25 days, with a cleanup maneuver performed at E- 10 days. The data arcs for the analyses arc bounded by the E-60 day maneuver and the data cut-off for the design of the E-10 day maneuver, which was at E- 16 days.

The data used in the analysis arc two-way Doppler and range received at all three of the DSN (Deep Space Network) ground station complexes, located in Goldstone, California,, Canberra, Australia, and Madrid, Spain. Additionally, delta-Differenced one-way Range (ADOR) is used. This data type consists of near-simultaneous delay measurements of radio signals from the spacecraft and a quasar, which are received at two stations forming an intercontinental baseline. This allows for a direct measurement of angular position of the spacecraft relative to the known position of the quasar.

THEORETICAL BACKGROUND

Sonic insight into the ability of range and Doppler measurements to determine the trajectory of a distant spacecraft can be obtained by analyzing the theoretical precision with which the geocentric spacecraft motion can be sensed from one or two tracking passes of data, Similar analyses have been performed previously for ranging and Doppler data separately [1 -3]. Two - way Doppler and range observations arc physically accomplished by measuring the phase of a carrier signal received from the spacecraft relative to a stable reference signal, in the case of Doppler, and by measuring the phase shift of a series of tones with different frequencies transmitted 10 and received from the spacecraft, in the case of ranging. In this discussion, it shall be assume.d that range and Doppler measurements arc equivalent to observations of the station-to-spacecraft range and range rate, respectivel y. A more detailed description of the actual Doppler and ranging systems used in the DSN is given by Kinman [4].

The station-spacecraft tracking geometry is illustrated in Fig. 1. The topocentric range, ρ, and range rate, $\dot{\rho}$, can be approximated over short periods of time (up 10 roughly 24 hr) in terms of the geocentric spacecraft range (r), range-ra[c ($\dot{r}$), declination (δ), and right ascension (α), as follows:

$$p \approx r - (r_s \cos(\delta) \cos(H) + z_s \sin(\delta)) \quad (1)$$

$$\dot{\rho} \approx \dot{r} + \omega\, r_s \cos(\delta) \sin(H) \quad (2)$$

where

r_s = station distance from Earth's spin axis (spin radius)

z_s = station height above Earth's equator (z-height)

ω = Earth rotation rate (7.3 x 10^{-5} rad/sec)

$H = \alpha_g + \lambda - \alpha$

and

α_g = right ascension of Greenwich meridian
λ = station east longitude

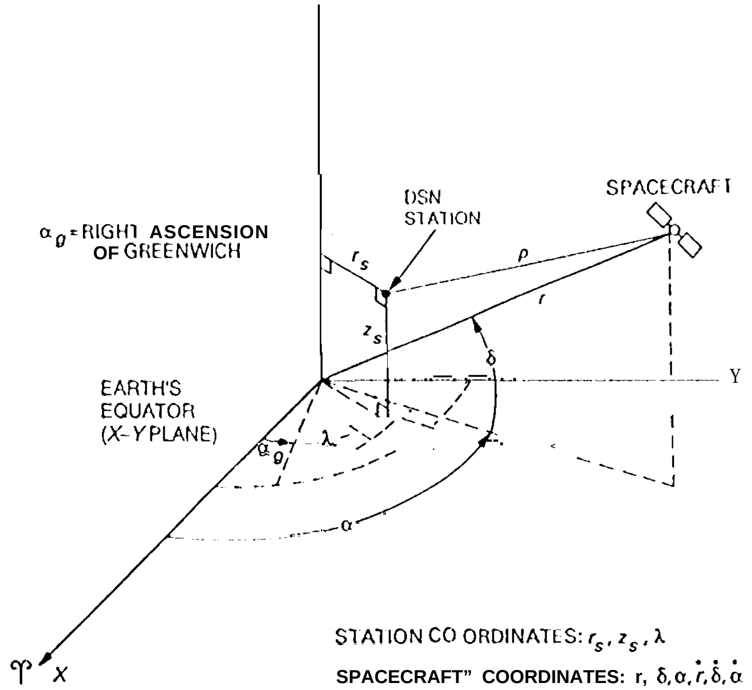

Figure 1: Station-spacecraft tracking geometry

From Eqs. (1) and (2), it can be seen that four of the six components of the geocentric spacecraft trajectory - r, $\dot{r}$, δ, and α -- can be sensed directl y by range and range rate measurements. Over the time period of interest, $\dot{r}$, δ, and α are nearly constant; determination of the remaining two coordinates, $\dot{\delta}$ and $\dot{\alpha}$, normally requires the acquisition of multiple passes of data over a period of several days. The accumulated information in each ranging and Doppler pass can be thought of as a multi-dimensional measurement of the spacecraft state, with the statistical combination of several of these "measurements" yielding a complete determination of the flight path. For data arc lengths exceeding one or two weeks, the parallax offered by the relative movement of the Earth and the spacecraft around the Sun also plays a significant role in ranging and Doppler-based navigation.

A simple least-squares error analysis of estimates of r, $\dot{r}$, δ, and α derived from a single pass of ranging and Doppler data can be formulated analytically (refer to the paper by Hamilton and Melbourne [3] for a detailed description). For the purposes of this analysis, it is assumed that, $\dot{r}$, δ, and α are constants, and that r varies linearly with time. The information matrix, J, for these coordinates, assuming a tracking pass in which the station-spacecraft hour angle H varies as $-\psi \leq H \leq +\psi$, can be expressed as

$$J = \left(\frac{1}{\sigma_\rho^2 \omega \Delta t}\right) \int_{-\psi}^{\psi} \left[\frac{\partial \rho}{\partial(r, \dot{r}, \delta, \alpha)}\right]^T \left[\frac{\partial \rho}{\partial(r, \dot{r}, \delta, \alpha)}\right] dH + \left(\frac{1}{\sigma_{\dot{\rho}}^2 \omega \Delta t}\right) \int_{-\psi}^{\psi} \left[\frac{\partial \dot{\rho}}{\partial(r, \dot{r}, \delta, \alpha)}\right]^T \left[\frac{\partial \dot{\rho}}{\partial(r, \dot{r}, \delta, \alpha)}\right] dH \tag{3}$$

where

σ_ρ = range measurement noise one-sigma uncertainty
$\sigma_{\dot{\rho}}$ = range rate (Doppler) measurement noise one-sigma uncertainty
Δt = time interval between measurements

In Eq. (3), it is assumed that Δt is the same for both the range and Doppler measurements. The partial derivatives appearing in Eq. (3) at some time t with respect to the geocentric coordinates at time t_0, where t_0 is assumed to be the time at which the spacecraft crosses the local meridian of the ground station, are as follows:

$$\frac{\partial \rho}{\partial(r, \dot{r}, \delta, \alpha)} = \left[1,\ t-t_0,\ r_s \sin(\delta) \cos(H) - z_s \cos(\delta),\ -r_s \cos(\delta) \cos(H)\right] \tag{4}$$

$$\frac{\partial \dot{\rho}}{\partial(r, \dot{r}, \delta, \alpha)} = \left[0,\ 1,\ -\omega\, r_s \sin(\delta) \sin(H),\ -\omega\, r_s \cos(\delta) \cos(H)\right] \tag{5}$$

Using Eqs. (4) and (5) to carry out the computations specified in Eq. (3) and inverting the information matrix yields the statistical variances for the geocentric range (σ_r^2), range rate ($\sigma_{\dot{r}}^2$), declination (σ_δ^2), and right ascension (σ_α^2) as follows:

$$\sigma_r^2 = \omega \Delta t\, f_1(\psi, r_s, z_s, \delta, \sigma_\rho^2, \sigma_{\dot{\rho}}^2) \tag{6}$$

$$\sigma_{\dot{r}}^2 = \omega \Delta t\, f_2(\psi, r_s, \delta, \sigma_\rho^2, \sigma_{\dot{\rho}}^2) \tag{7}$$

$$\sigma_\delta^2 = \frac{\omega \Delta t}{(r_s \sin \delta)^2} f_3(\psi, \delta, \sigma_\rho^2, \sigma_{\dot{\rho}}^2) \tag{8}$$

$$\sigma_\alpha^2 = \frac{\omega \Delta t}{(r_s \cos \delta)^2} f_4(\psi, \sigma_\rho^2, \sigma_{\dot{\rho}}^2) \tag{9}$$

Eqs. (6)-(9) are similar to expressions derived by Anderson [4] in an earlier analysis of this same problem (the functions f_1 through f_4 are not shown explicitly, as they are fairly complex). Eq. (8), in particular, predicts that the declination of a spacecraft crossing the celestial equator ($\delta = 0$) cannot be sensed, although this indeterminacy is not rigorously correct, but is rather an artifact of the approximations used in Eqs. (1) and (2). In contrast, σ_α is seen from Eq. (8) to be proportional to $1/\cos\delta$, which has little ($\pm$10 percent) variation over the declination range spanned by the ecliptic plane ($\pm$24 degrees), in which most interplanetary spacecraft trajectories lie.

The situation described above changes dramatically when an additional pass of ranging and Doppler data from a properly chosen second station is added into the information matrix. Consider a scenario in which a tracking pass is acquired from a station with z-height z_s and spin radius r_s, followed immediately by another pass from another station with z-height $-z_s$ and spin radius r_s (Fig. 2). This choice of station coordinates is actually a good approximation for stations located at the DSN sites at Goldstone, California and near Canberra, Australia, which have spin radii that are nearly equal (to within about 5 km) and z-heights that are nearly equal in magnitude but have opposite signs. Using Eqs. (3)-(5) to compute an information matrix for the first pass, then adding this matrix to an information matrix for the second pass and inverting the sum yields a covariance matrix for the combined information contained in both passes. This procedure yields a formula for σ_δ^2 of very simple form when $\delta = 0$:

$$\sigma_\delta^2 = \frac{\sigma_\rho^2}{4 z_s^2}\left(\frac{\omega \Delta t}{\psi}\right) \tag{10}$$

Equation (10) indicates that the z-height component of the baseline formed by the two stations enables a determination of δ, and that this determination is provided solely by the ranging data. The result for σ_α^2 obtained in the two station case is just the expression in Eq. (9) multiplied by a factor of 1/2. With typical S-band ranging and Doppler data accuracies of 5 to 10 m and 0.3 to 1.0 mm/s, respectively, for measurements acquired at intervals of a few minutes, Eqs. (9) and (10) predict that the angular coordinates of a spacecraft can be sensed with a precision of roughly 0.1 to 0.35 µrad for pass lengths of 8 to 12 hr (ψ = 60 to 90 degrees). In comparison, the theoretical angular precision of S-band ΔDOR, which was also used to obtain angular measurements during Galileo Earth encounter navigation operations, was about 0.04 to 0.08 µrad, depending upon the tracking geometry.

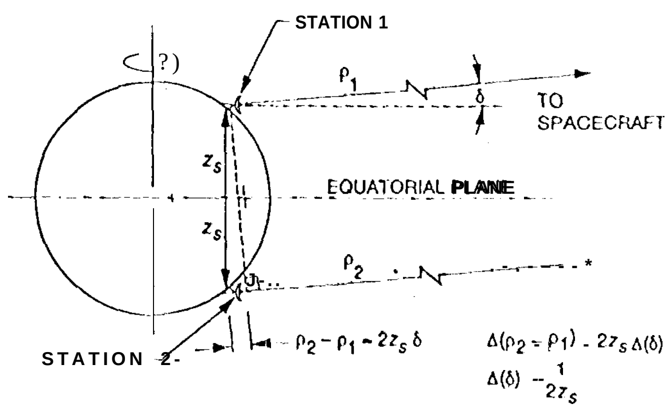

Figure 2: Declination determination using range measurements from two widely separated stations

While the theoretical results above snow that ranging can overcome the dependence of IJopplcr-based angle determination on the spacecraft declination, it must be recognized that the effects of systematic range measurement errors, principally station delay calibration errors and charged particle (Earth ionosphere and solar plasma) calibration errors, will not necessarily be reduced by averaging, as will the effects of random error sources. These systematic errors must be accounted for in some way, or reduced *a priori* through the use of highly accurate calibrations.

FILTER STRATEGY

To account for the effects of systematic bias errors on the ranging data, independent bias parameters arc modeled for each station pass, This strategy allows the orbit determination filter to estimate errors duc to miscalibration of the ground system hardware. Additionally, these bias parameters can also be used to approximately account for slowly varying transmission media effects, such as solar plasma delay. These effects, although not truly constant over a pass, vary slowly enough that the major portion of the effect can be modeled as a bias. This simple ranging error model was implemented by estimating a stochastic bias for each ranging pass in the data arc, using a batch-sequential filter.

The *a priori* uncertainty of these bias parameters was chosen to be 5 m. This value was chose.n as to allow the filter to estimate both transmission media effects as well as errors duc to the calibration of the ground systems. in fact, examination of the values for the station delay calibration (performed prior to each ranging pass) during the E1 approach found an RMS variation of the calibrations of only 55 cm. The stability of the station calibrations during the E2 approach was similar. A complete summary of the filter assumptions used can be found in '1'able 1.

EARTH-1 ANALYSIS AND RESULTS

The E1 data arc extends from Iii-59 days to E1-15 days. (10 October 1990 to 23 November 1990). During this time the Earth-spacecraft distances ranged from 50 [o 12.5 million kilometers and the geocentric declination varied from 15 to 13 degrees. During this period, 3740 Doppler observations (600 scc count time) and 2750 range observat ions were obtained. Nineteen ADOR observations were performed, 11 of (hen} utilizing the Goldstone-Canberra baseline and the remainder utilizing the Goldstone-Madrid baseline. A standard Doppler weight (one-sigma measurement uncertainty) of 1 mm/s (for a 60 scc count) was used and the range weight was . varied, from ten meters to two meters. The data weight used for the ADOR data was 50 cm.[4] A series of solutions were performed, These included Doppler only, and Doppler and range with various range weights (100, 10m, and 2 m), and a solution using Doppler, range, and ADOR, This final solution closely corresponds to what was used for the operational design of the final maneuver. l'able 2 summarizes the solutions performed,

Figures 3 and 4 shows all of the solutions in the E1 encounter aiming plane (scc Appendix). Figure 3 shows all of the traditional runs, while Figure 4 shows the precision range filter strategy solutions compared to the best traditional solution. The thi rd component, the linearized time of flight, was the same for all strategies and is therefore not shown. All of these solutions arc compared [0 the post-flyby reconstruction. This reconstruction is accurate to the 100 m level. The best result is from the 5 m range weight solution, although both the S m and 10 m solutions provide solutions which are comparable to that provided by the ADOR solution. All of the range solutions provide considerable improvement over the Doppler only solution. The two meter range weight solution, however, dots not possess uncertainties that arc any better than

[4]This is a differential delay observation converted 10 units of length. This data weight corresponds to an angular position of 75 nanoradians on the. Goldstone-Madrid base.line and 50 nanoradians on the Goldstone-Canberra baseline.

the 5 m or 10 m weight solutions. The movement of this solution is caused by the weighting of the data beyond that which is warranted by the data quality. Although the post-fit RMS of the range residuals in all of the precision range solutions is approximately 1 m over the entire data arc, the residuals are much larger than this for the early part of the data arc where the ranging sigtlal-to-noise ratio (which varies as $1/r^4$) was much smaller, yielding substantially larger thermal noise levels. The 5 m range weight solution and the 10 m range weight solution arc in error by 0.48 μradians and 0.37 μradians, respectively.[5] This compares with an error of 0.76 μradians for the best solution using the conventional filler strategy.

Source	A priori 1-σ	Remarks
Random Data Noise Doppler (60-sec average) Range	1 mm/s 100m to 2 m	One way equivalent data weights
Estimated Parameters		
Spacecraft State Vector	position: 10^8 km velocity: 10^8 km/s	No a priori information assumed
Solar Radiation Pressure coefficients	radial 5% transverse 1 %	Expressed as percentage of nominal acceleration
Attitude update maneuvers	0.5 mm/s (spherical)	Approximately 1 every 2 weeks
Propellant Line flushings	Magnitude: 0.5 mm/s Direction: 15 mrad	Approximately 1 every 3 weeks
Quasar location for ΔDOR	100 nanoradians	conservative
Estimated Stochastic Parameters		
Range Biases (one per station-pass)	5 m	
Consider Parameters (parameters not included in the filter estimates, but included in the final uncertainties)		
Earth GM	0.15 km^3/s^2	JPL ephemeris DE 125
Earth Ephemeris (Heliocentric)	Radial: TITEFP Along track: 30.0 km Out of Plane: 1S.0 km	JPL ephemeris DE 125
DSN station Locations	spin radius: 0.24 m longitude: 0.24 m z-height: 0.30 m	The relative uncertainty between stations is approximately 5 cm,
Spacecraft accelerations	transverse: 1×10^{-12} km/s	
Tropospheric zenith Delay	4 cm 1 cm (dry)	
Ionospheric zenith Delay	75 cm (day) 15 cm (night)	S-band values (conservative)

Table 1: Modeling Assumptions

[5] Geocentric angular error at the end of the data arc

Figure 5 snows the results of the solutions for the stochastic range biases and their associated 1 σ uncertainties. It can be seen that the *a posteriori* uncertainty of the estimates does improve by approximately a factor of two in comparison 10 the ***a priori*** uncertainty of 5 m. Both single pass outliers as wc]] as long term [rends arc present. This indicates that the filter is solving for both station calibration errors (single pass) and longer term phenomena (most likely solar plasma effects).

Solution	Data Types and Weight			Comments
	Doppler	Range	ADOR	
1	1 mm/s	N/A	N/A	No stochastic range biases estimated
2	1 mm/s	100 m	N/A	No stochastic range biases estimated
3	1 mm/s	10 m	N/A	New filter strategy used
4	1 mm/s	5 m	N/A	New filter strategy used
5	1 mm/s	2 m	N/A	New filter strategy used
6	1 mm/s	100 m	50 cm	No stochastic range biases estimated

Table 2: Summary of' Solutions

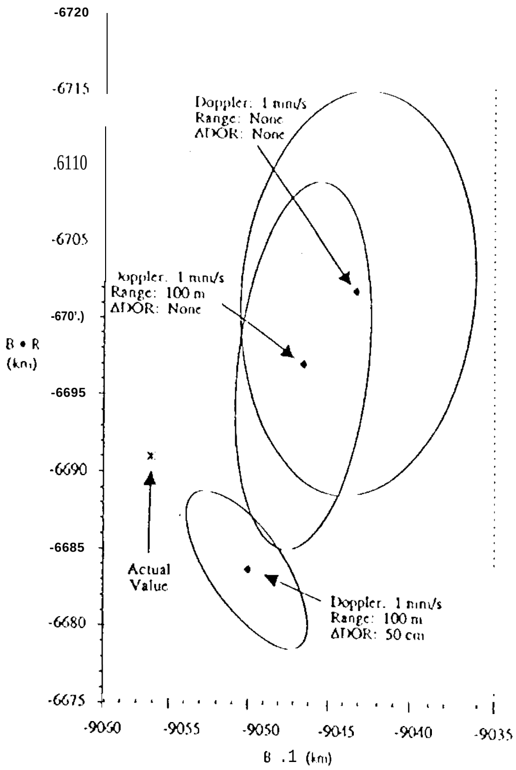

Figure 3: E1 Conventional Solutions

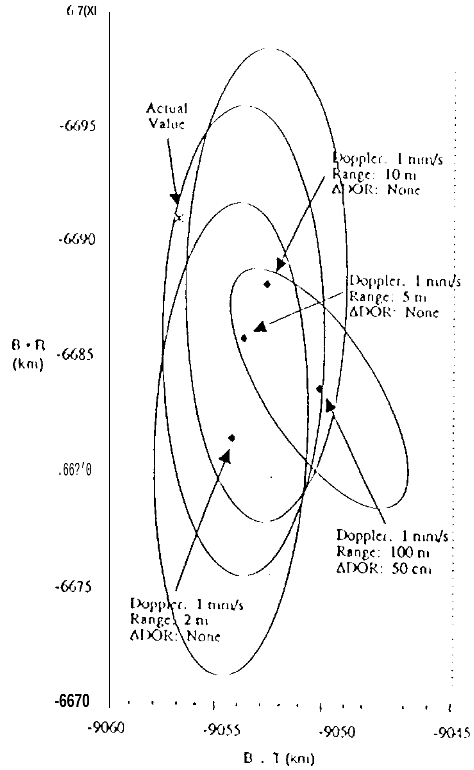

Figure 4: E1 High Precision Range Solutions

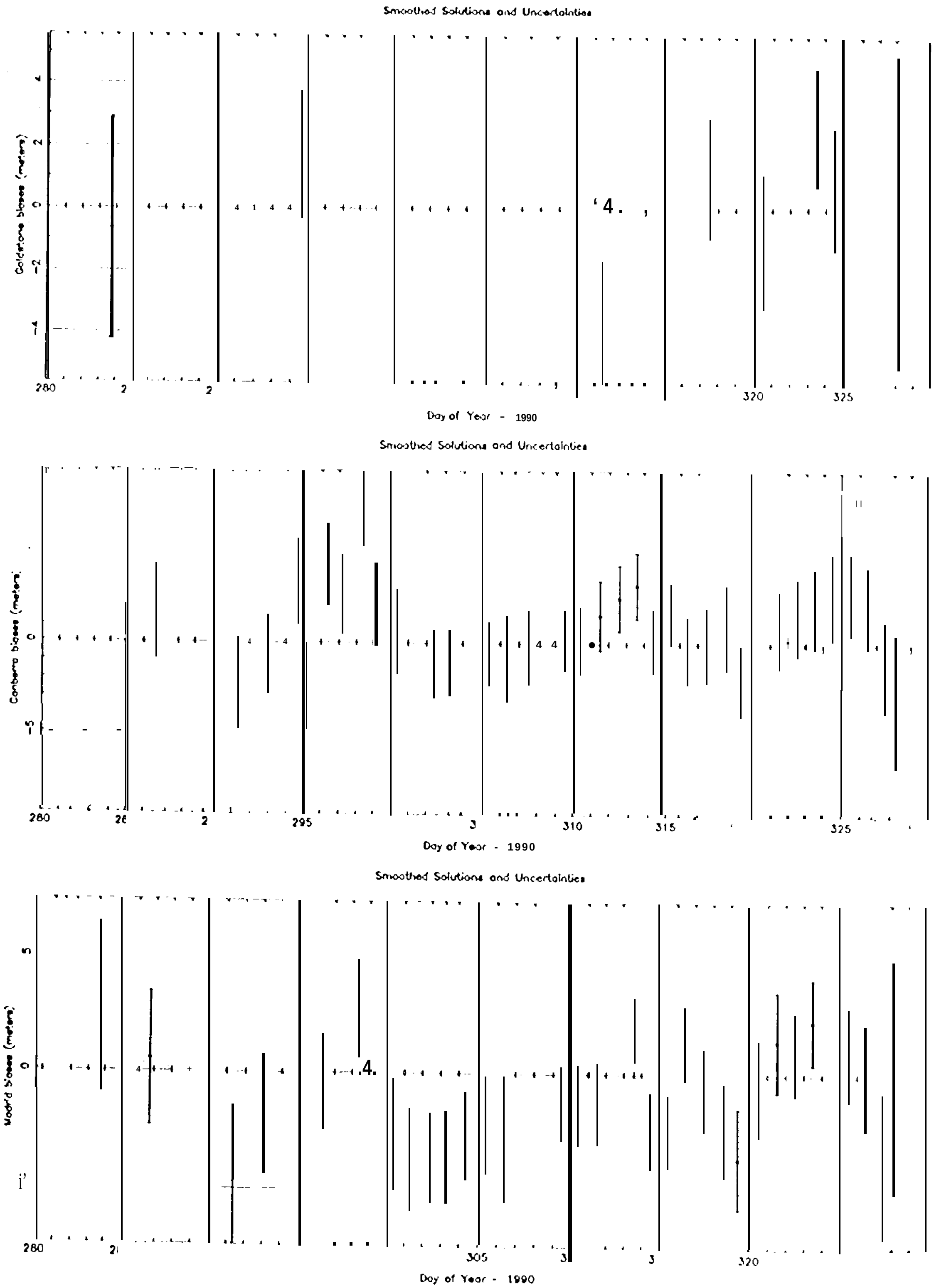

Figure 5: E1 Range Bias solutions and Uncertainties

EARTH-2 ANALYSIS AND RESULTS

The second flyby of Earth in December of 1992 was similar to the first in many aspects. Both flybys were achieved by a series of targeting mane.uvcrs placed at Earth-60 days, Earth-25 days and Earth- 10 days, Continuous tracking started 35 days prior to closest approach, and a campaign of ADOR observations supplemented the collection of Doppler and range data. "1'here were, however, some di fferences between the two flybys worth noting, For one, the spacecraft was much higher in geocentric declination for the second flyby (300 versus 13°). Also, the second flyby resulted in an altitude of 304 km at closest approach, rather than the 960 km altitude at the first flyby. This final difference, however, had no significant effect on the precision range investigation.

The data arc for the second flyby was slightly different from the first for two reasons. For the E1 analysis, the data arc started immediately after the Earth-60 maneuver. This could not be done in the Earth-2 case duc to an attitude change 5 days after the Earth-60 day maneuver.~ Due to the size. of this turn and its effect on the orbit determination process, it was decided to start the data arc for the E2 investigation after this turn. This, combined with a data cutoff a day earlier, (for ground sequencing reasons) made the Earth-2 data arc 6 days shorter than that for E1 Secondl y, duc to heavy competition for DSN station time from November 6-14, fewer ranging opportunit ics than in the E1 case were available. Overall, the E2 data arc contains 2260 Doppler points (600-second count time) and 1834 range. points from October 15 to November 22. In addition to the radiometric data, 2.1 ADOR observations were attempted from October 27 to November 21, resulting in 9 usable ADOR observations from the Goldstone-Canberra baseline and 1() from the Goldstone-Madrid baseline. The list of estimated and considered parameters and their *a priori* uncertainties for those parameters arc identical to that used in the E1 analysis. ('I'able 1). Doppler was weighted at 1 mm/sec (for a 60-second count) and range was weighed at 100 m, 10 m , 5 m. and 2 m, exactl y as in the E1 investigation.

The results of the E2 analysis arc shown in Figures 6 and 7. As was done for the E1 experiments, all results were mapped to the Earth-centered aiming plane at the time of c1oscsL approach. As was true for E1, the aiming plane was nearly coincident with the plane-of-sky, which meant the ability of each strategy to determine the aim point for the encounter was closely related to the ability to determine the geocentric angular position of the spacecraft over the data arc. All solutions arc Compared to the post-flyby reconstruction. Figure 6 shows the aiming plane results from the more traditional data fitting techniques, while Figure 7 shows solutions produced via the precision range filter. The 1 -sigma uncertaint y ellipses are also shown for each solution. In every case, the solution was within 1-sigma of the true solution. Of all solutions shown in Figure 6 the Doppler-range-AIXIR case was the best with an error of 1.6 km in the B-plane.

Of the three solutions shown in Figure 7, the 2 meter solution yields the best estimate, with an error of 2.5 km in the aiming plane. This number corresponds to an angular accuracy of 0.16 μrad at 16 days before c1oscsI approach, which is consistent with {he. theoretical angle finding precision of the ranging data. Because of the high declination situation in Earth-2, the Doppler solution is a strong onc to begin with. Therefore, the true strength of the precision ringing technique only comes into play when the range is weighted better than 5 meter accuracy. The improvement in the 2 m solution as compared to the performance of a 2 m weight solution from E1 was expected, as most of the ranging data obtained for E2 was acquired over smaller distances than El, resulting in a smaller thermal noise level in the data. The range data quality at E2 was twice that of E1, with a post-fit RMS for the range residuals of 50 cm.

[6] This was a 40° attitude change. associated with an attempt to deploy the High Gain Antenna. The effect of ibis attitude change is not separable from the maneuver just prior.

Figure 8 show the results of the range bias solutions for the 2 m range weight solution. Ranging from all three stations, especially Goldstone, during the early part of November was sparse due to conflicts with other projects and activities for station tracking and calibration time. Continuous ranging was available on day 318, and gaps after that date are where the range data was deleted due to unusable station calibration data. The largest range bias value of 50 range units (7.2 meters) occurred at Madrid on DOY 289, and when compared with a range residuals display for a 100 meter range fit, could be explained as an unusually large station calibration error for that day. Where the range data was near-continuous, there is some slight correlation in all three stations (seen as a downward slope from day 320 to day 325). Since the behavior is similar for all three stations, it suggests the filter is detecting range delay variations induced from non-station sources, such as the effect of solar plasma, or perhaps the spacecraft transponder electronic delay.

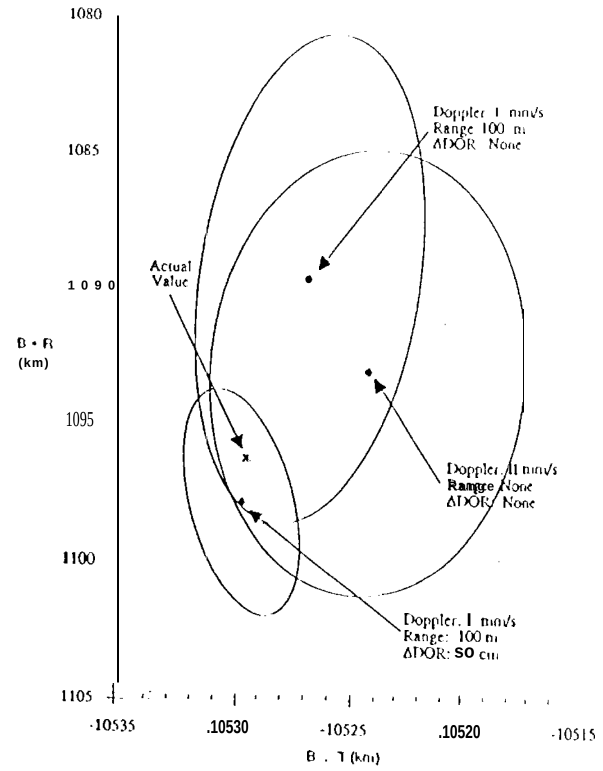

Figure 6: E2 Conventional Solutions

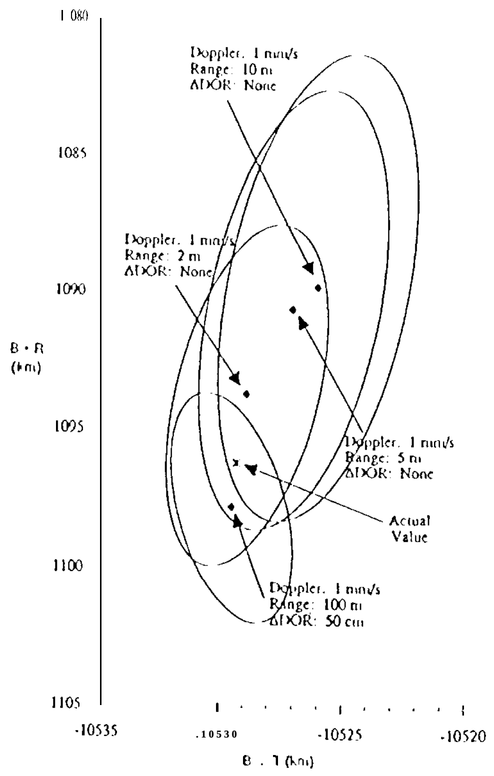

Figure 7: E2 High Precision Range Solutions

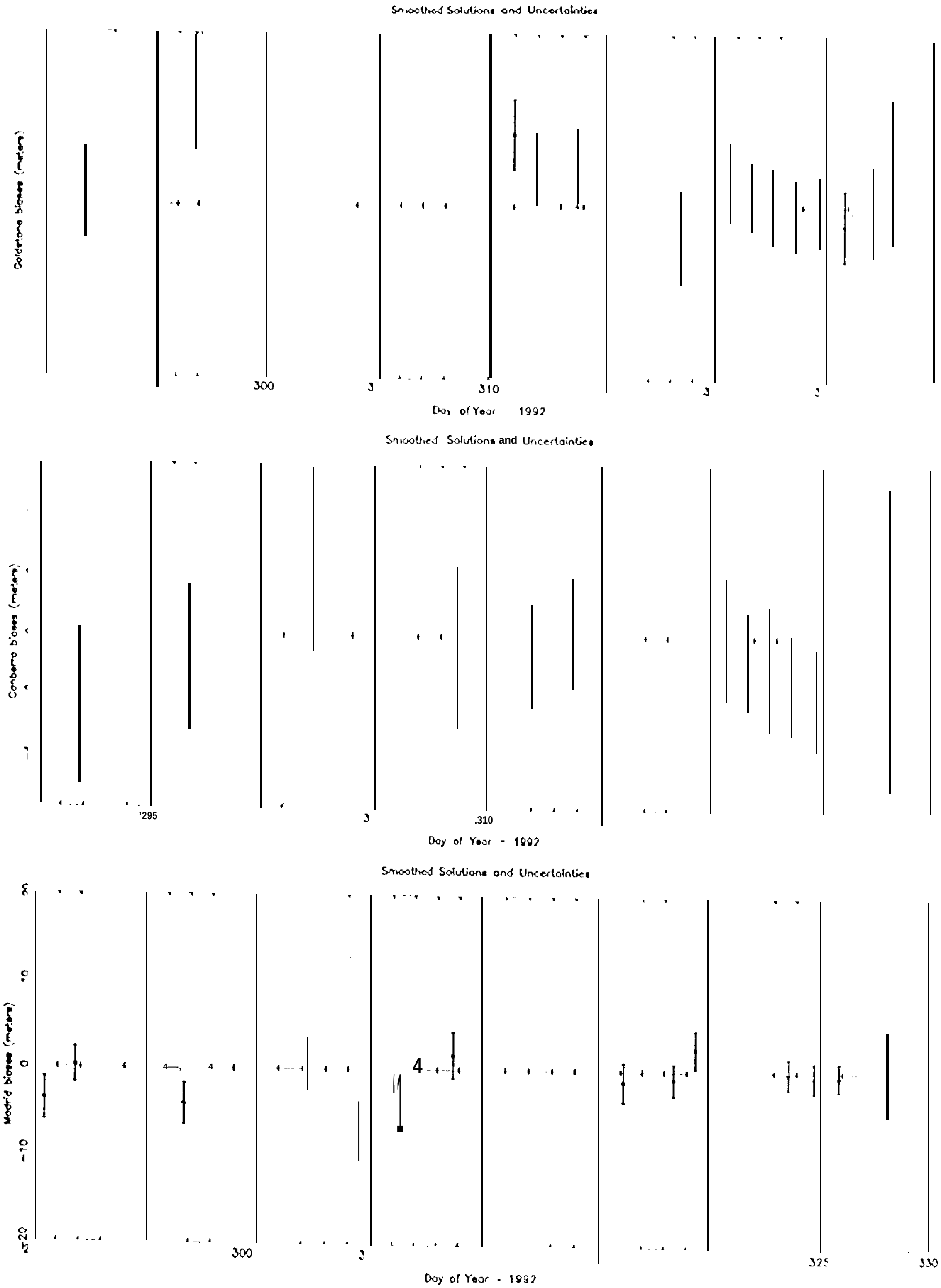

Figure 8: E2 Range Bias Solutions and Uncertainties

CONCLUSIONS

The E1 and E2 orbit determination analysis results are similar in many respects. In both cases, the performance of the precision range filter strategy yielded solutions comparable to or better than those obtained using ADOR, although in theory ADOR provides more accurate angular position measurements. The relatively poor performance of the conventional solutions using ADOR is attributed to the relative sparseness and irregular distribution of the ADOR data set. This is in turn due to the operational requirements associated with obtaining ADOR observations, which preclude as frequent an acquisition of observations as Doppler and range. The relative ease of ranging data acquisition and processing makes ranging an attractive alternative to ADOR when the precision of the ADOR observations are not required.

ACKNOWLEDGMENTS

The authors wish to acknowledge lilt valuable contributions and suggestions received from '1'. P. McElrath and R. A. Jacobson. The work described in this paper was carried out at the Jet Propulsion Laboratory, California Institute of Technology, under contract with tile National Aeronautics and Space Administration.

REFERENCES

1. Thurman, S. W., McElrath, '1'. 1'., and V. M. Pollmeier, "Short-Arc Orbit Determination Using Coherent X-Band Ranging Data," Paper AAS-92-109, AAS/AIAA Spaceflight Mechanics Meeting, Colorado Springs, Colorado, 24-26 February 1992.

2. Hamilton, T. W., and W. G. Melbourne, "Information Content of a Single Pass of Doppler Data from a Distant Spacecraft," *JPL Space Programs Summary .?7-.?9, Vol. 1//,* March-April 1966, pp. 18-23.

3. Anderson, J. D., "The Introduction of Range Data into the Data Compression Scheme," *JPL Space Programs Summary 37-43, Vol. ///,* November-December 1966, pp. 18-24.

4. Kinman, P. W,, "Doppler Tracking of Planetary S pacecraft," *IEEE Transactions on* Microwave *Theory and Techniques*, Vol. 40, No. 6, pp. 1199-1 204, June 1992..

APPENDIX

Planctary approach trajectories arc typically described in aiming plane coordinates, often referred to as "1~-plane" coordinates (scc Fig. A-1). The coordinate system is defined by three orthogonal unit vectors, $\underline{S}$, $\underline{T}$, and $\underline{R}$ with the system origin taken to be the center of the target planet. The $\underline{S}$ vector is parallel to the spacecraft's approach asymptote (parallel 10 [tic V_∞ vector) while $\underline{T}$ is orthogonal to S and lies in the ecliptic plane. Finally, $\underline{R}$ completes an orthogonal triad with $\underline{S}$ and $\underline{T}$

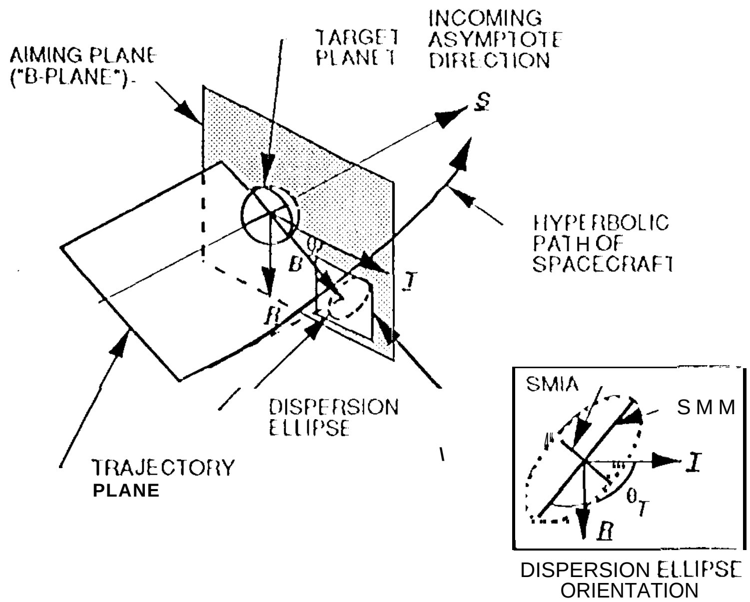

Fig. A-1 Aiming l'lane Coordinate System Definition

The aim point for a planctary encounter is defined by the miss vector, B, which lies in the& $\underline{R}$ plane, and specifics where the point of closest approach would be if the spacecraft's flight path were not deflected by the gravity of the target body. The time from encounter (point of closest approach) is characterized by the *linearized time-of-flight (1 ,TOF)*, which speci fits what the time of flight to encounter would be if the magnitude of the miss vector were zero. Orbit determination errors arc characterized by a one-sigma or three-sigma II-plane dispersion ellipse, also shown in Fig. A-1, and the one-sigma or three-sigma uncertainty in LTOF. in Fig. A-1, SMIA and SMAA denote the semi-mil~or and semi-major axes of the dispersion ellipse, respectively.